Combined inhibition of KDM6A/B and HDACs exacerbates integrated stress response and mediates therapeutic effects in *IDH1*-mutant glioma

Alisan Kayabolen[1], Gizem Nur Sahin[2], Fidan Seker-Polat[1], Ahmet Cingoz[1], Bekir Isik[1], Simge Acar[1], Hiroaki Wakimoto[3], Daniel P. Cahill[3], Ihsan Solaroglu[4], Adam Cribbs[5], Udo Oppermann[5,6,7,*], Tugba Bagci-Onder[1,*]

[1]Brain Cancer Research and Therapy Lab, Koç University School of Medicine, Istanbul, 34450, Turkey
[2]Department of Histology and Embryology, Koç University School of Medicine, Istanbul, 34450, Turkey
[3]Department of Neurosurgery, Massachusetts General Hospital Cancer Center, Harvard Medical School, Boston, Massachusetts, 02114, USA
[4]Department of Neurosurgery, Koç University School of Medicine, Istanbul, 34450, Turkey
[5]Botnar Research Centre, NIHR Biomedical Research Centre Oxford, University of Oxford, OX3 7LD, UK
[6]Structural Genomics Consortium, University of Oxford, OX3 7DQ, UK
[7]FRIAS, Freiburg Institute of Advanced Studies, University of Freiburg, 79104, Freiburg, Germany

* Corresponding authors
Koç University School of Medicine,
Koç University Research Center for Translational Medicine
Rumelifeneri Yolu, 34450, Sariyer, Istanbul, TURKEY
E-mail: tuonder@ku.edu.tr, udo.oppermann@sgc.ox.ac.uk,

Running title: Epigenetic inhibitor combination to target *IDH1* mutant glioma

Word count: 7323

ABSTRACT

IDH1/2-mutant gliomas are primary brain tumors for which curative treatments are lacking. Using a chemical screen targeting chromatin modifiers, we identified the histone H3 K27me3 demethylase inhibitor GSK-J4 and class I histone deacetylase inhibitors such as Belinostat as potent, genotype-selective agents against *IDH1*-mutant glioma. RNA-sequencing on paired wild-type and *IDH1*^{R132H} cells revealed induction of stress-related pathways in *IDH1*^{R132H} cells, which was dependent on the onco-metabolite 2- hydroxyglutarate (2-HG). GSK-J4 and Belinostat combination activated an ATF4-mediated integrated stress response, cell cycle arrest, and *DDIT3*/CHOP-dependent apoptosis in *IDH1*-mutant cells. We show that genetic ablation of GSK-J4 target histone demethylases, KDM6A and KDM6B phenocopied the pharmacological effects of the compound. Combination treatment of GSK-J4 and Belinostat extended animal survival in an *IDH1*-mutant orthotopic model *in vivo*. These results provide a possible therapeutic approach that exploits epigenetic vulnerabilities of *IDH*-mutant gliomas.

Keywords: *IDH* mutation, glioma, epigenetic, stress response, combination therapy

Statement of Significance:

IDH1/2 genes are frequently mutated in low grade glioma and secondary glioblastoma. These tumors exhibit a distinct epigenome with increased DNA and histone methylation; therefore, identifying and exploiting their epigenetic vulnerabilities may lead to effective therapies. We discover targeting of KDM6A/6B together with HDACs provides a promising genotype-specific therapeutic approach.

INTRODUCTION:

Glioblastoma is the most malignant glioma type with an average patient survival of 14-16 months despite surgery and chemo-radiation[1]. Glioblastomas can arise *de novo*, or they can progress from lower grade gliomas (LGG). Although the survival rate is higher in LGGs, most LGGs eventually progress to high-grade glioma, known as secondary glioblastoma. In an integrated genomic analysis from The Cancer Genome Atlas (TCGA), it was shown that a small subset of glioblastoma samples carried a point mutation in *Isocitrate Dehydrogenase* (*IDH1)* gene[2]. Further analyses revealed that the *IDH1* mutation is found in 70-80% of LGGs and secondary glioblastomas[3]. Mutations are exclusive at position 132 in *IDH1* or position 172 in *IDH2* genes, corresponding to the enzymes' active sites responsible for converting isocitrate to alpha-ketoglutarate (2-oxoglutarate, 2-OG)[3]. Point mutations in *IDH1* or *IDH2* lead to a gain of function of the enzyme. Mutant IDH converts 2-OG produced by the wild-type IDH enzyme, into 2-hydroxyglutarate (2-HG) [4]. 2-HG antagonizes the activities of several 2-OG dependent enzymes, such as TET enzymes or KDMs which are DNA and histone demethylases, respectively[4]. Therefore, IDH mutation leads to hypermethylation of both DNA and histones generating a distinct epigenetic profile called glioma CpG island methylator phenotype (G-CIMP)[5].

Based on clonal evolution analyses in tumor samples, IDH mutation is classified as a driver mutation in LGG, since it is among the earliest genetic events in tumorigenesis[6]. Therefore, inhibition of mutant IDH with specific inhibitors is explored as a strategy to delay tumor growth and prevent tumorigenic effects of 2-HG[7,8]. Reversing altered chromatin structure with DNMT inhibitors is also offered as another strategy for *IDH*-mutant gliomas[9,10]. On the other hand, *IDH*-mutant cells have been shown to grow slower than wild-type cells. A distinct metabolic profile via altered TCA cycle[11], and modulation of mTOR and ATP synthase activities[12], are considered as potential causes for the slow growth of *IDH*-mutant glioma cells. In addition, recent work has indicated that 2-HG produced by mutant IDH leads to suppression of DNA repair through local chromatin dysregulation[13]. Based on these metabolic and epigenetic perturbations, exploiting the vulnerabilities of *IDH*-mutant cells by inhibiting crucial pathways has been proposed as a possible therapeutic strategy[14–17]. Taken together, there is considerable interest in selective targeting of *IDH*-mutant cancers.

Therapeutic targeting of *IDH*-mutant gliomas is mostly centered around using specific mutant IDH enzyme inhibitors[7,8]. However, an alternative strategy may be to take advantage of the distinct metabolic and epigenetic phenotypes of *IDH*-mutant gliomas and identify vulnerabilities associated with these altered cellular states. In this study, we interrogated the epigenetic vulnerabilities of primary *IDH1*-mutant glioma cells through a chemical screen targeting several chromatin modifiers. We established that the combination of GSK-J4, a histone H3K27me3 demethylase inhibitor, and Belinostat, a class I histone deacetylase inhibitor, has synergistic cytotoxic effects on *IDH1*-mutant glioma cells. This selective vulnerability of *IDH1*-mutant glioma cells involved the activation of an integrated stress response (ISR) and an apoptotic program.

RESULTS:

Epigenetic inhibitor screen identifies potent compounds targeting *IDH1*-mutant gliomas

We conducted a chemical screen in two independent primary glioma cell lines, MGG119 and MGG152, that carry a R132H point mutation in *IDH1*[18]. We employed a focused library composed of 46 compounds targeting different classes of chromatin modifiers and assessed the overall viability of cells in response to treatment with a single dose of chemicals (**Figure 1A**). DMSO-only treated and untreated cells served as negative controls. On average, most compounds had minimal effect on cell viability (reducing viability to 92.4±15.3% for MGG119, and to 86.7±21.7% for MGG152) (**Figure 1B**). We considered a compound a "hit" if it reduced cell viability 1 SD or lower (77.1% and 65.0%, respectively) in both cell lines. Accordingly, 5 compounds significantly decreased the viability of both MGG119 and MGG152 cells, namely 5-azacytidine; a DNA methyltransferase (DNMT) inhibitor, Chaetocin; an unspecific lysine-methyltransferase (KMT inhibitor), GSK-J4; a histone H3K27me3 demethylase inhibitor, and Belinostat and Trichostatin A, class I histone deacetylase (HDAC inhibitors). Treatment of glioma cells revealed dose-dependent effects of these compounds on both cell lines (**Figure 1C**). Two independently derived non-malignant human fibroblast lines (Fibro1 and 2), were significantly less affected by GSK-J4 or HDACi, suggesting a high degree of selectivity of the chosen compounds (**Figure 1C**).

To examine the combinatorial efficacy of the selected compounds, we applied possible dual combinations of 4 screen hits targeting different types of chromatin modifiers on *IDH1*-mutant cells or fibroblasts (**Figure 1D**). To this end, we chose compound concentrations that did not markedly reduce tumor cell viability. Fibroblasts were not affected from the treatment with compounds applied individually or in combination; however, *IDH1*-mutant glioma cells displayed significantly reduced viability upon combination treatments **(Figure S1A-D),** as illustrated as a heat map of the viability results (**Figure 1E**). Specifically, "5-azacytidine + Chaetocin" and "GSK-J4 + Belinostat" combinations reduced the viability of glioma lines, without majorly affecting fibroblasts (**Figure 1F**). Indeed, the highest efficacy was demonstrated with the combination of GSK-J4 and Belinostat. Their effects were synergistic on *IDH1*-mutant tumor cells **(Figure S1E-F),** but not on human astrocytes (**Figure S3F).**

IDH1^{R132H} overexpression leads to global transcriptome alterations that are reversible with GSK864, an inhibitor of IDH^{R132H}

To examine the specific effects of *IDH1* mutation on the response of *IDH1*-mutant glioma cells to epigenetic inhibitors, we generated a paired cell line via overexpression of mutant IDH1^{R132H} in A172 cells. Immunohistochemical staining and Western blot analysis using an antibody specific to mutant IDH1 enzyme, confirmed the expression of mutant IDH1 (**Figure 2A, 2B**). The production of 2-HG was pronounced in the A172 *IDH1^{R132H}* cells, which could be reversed by 3-day treatment with GSK864, an inhibitor of mutant IDH1 enzyme **(Figure 2C).** We observed that *IDH1^{R132H}* cells grew slower than wild-type cells, which was also reversible with GSK864 treatment (**Figure 2D**). To further examine the molecular

differences between wild-type and *IDH1*^{R132H} cells, we assessed their transcriptome differences by RNA sequencing. Cells were grown with or without GSK864 prior to sequencing in order to dissect out mutant IDH1-driven differences between them **(Figure 2E).** *IDH1*^{R132H} cells displayed a high number of differentially expressed genes (DEGs) when compared to wild-type cells. Specifically, 463 genes were differentially expressed between wild-type and *IDH1*^{R132H} cells (|log2|>1, p<0.05), and the number of DEGs was markedly reduced (86 DEGs) in the presence of GSK864 **(Figure S2A, S2B)**. Importantly, wild-type cells were not affected by GSK864 treatment as there were only 2 DEGs in the comparison of wild-type cells that were either untreated or GSK864-treated (**Figure S2A, S2B**). Heat maps and cluster diagrams revealed that while the greatest degree of differential expression was between the wild-type and *IDH1*^{R132H} cells, upon GSK864 treatment, the transcriptomic profile of *IDH1*^{R132H} cells closely resembled that of wild-type cells (**Figure 2E, 2F**). qRT-PCR analysis confirmed the upregulation or downregulation of selected genes in the *IDH1*^{R132H} cells, which were reversible with GSK864 treatment (**Figure 2G, Figure S2C, S2D**). Interestingly, Gene Set Enrichment Analysis (GSEA)[19] revealed several hallmark pathways that were activated in *IDH1*^{R132H} cells compared to wild-type cells, such as inflammation-related "Interferon alpha response", "TNFa signaling via NFKB", "Interferon gamma response", "Inflammatory response", as well as cell stress-related "Hypoxia", "P53 pathway", and "Unfolded protein response" (**Figure 2H, 2I).** Importantly, the enrichment of these pathways was reversed in the presence of GSK864 in *IDH1*^{R132H} cells (**Figure 2H).** These results indicated that the A172 wild-type and A172 *IDH1*^{R132H} cell line pair provided a suitable model to study the effects of IDH1 mutation in glioma. We therefore tested the epigenetic inhibitors on this cell line pair and observed that *IDH1*^{R132H} cells were equally sensitive to 5-azacytidine or Chaetocin as wild-type cells. However, *IDH1*^{R132H} cells were significantly more sensitive to GSK-J4 or Belinostat than A172 wild-type cells **(Figure 2J).** This was also evident in another cell line pair that were established similarly, namely LN18 wild-type and LN18 *IDH1*^{R132H} cells **(Figure S3A-S3C).** Together, these results demonstrate genotype-selective vulnerability of *IDH1*^{R132H} cells to GSK-J4 or Belinostat treatment.

GSK-J4 and Belinostat combination selectively targets *IDH1*^{R132H} glioma cells

We next assessed the combinatorial efficacy of GSK-J4 and Belinostat in *IDH1*^{R132H} glioma cells using the established paired cell lines. A combination of GSK-J4 and Belinostat significantly reduced the viability of *IDH1*^{R132H} cells in a synergistic manner. In contrast, no synergistic effect of the compounds was observed in wild-type cells (**Figure 3A, 3B, Figure S3D).** To further monitor the differential effects of GSK-J4 and Belinostat on wild-type and *IDH1*^{R132H} cells, we utilized a live cell imaging system in a window of 96hrs after treatment (**Figure 3C, Supplementary videos 1-8)**. Quantification of the number of live cells at 0h, 24h, 48h, 72h and 96h demonstrated that *IDH1*^{R132H} cells were markedly more vulnerable to GSK-J4 and/or Belinostat treatment than wild-type cells (**Figure 3D**). While GSK-J4 or Belinostat mono-treatment halted growth of *IDH1*^{R132H} cells, the combination of both compounds led to a significant induction of cell death and a complete eradication of tumor cells at 72 hours (**Figure 3D**). These potent and selective effects of GSK-J4 and/or Belinostat treatment on A172 *IDH1*^{R132H} cells were further investigated with co-culture

experiments of tumor cells and fibroblasts (**Figure 3E)**. After treatment of co-culture of mCherry-labelled A172 *IDH1*^{R132H} cells and GFP- labelled Fibro1 cells with the compounds for 5 days, fibroblasts remained viable under all conditions, whereas A172 *IDH1*^{R132H} cells were significantly reduced in number (**Figure 3F**). Interestingly, the selective sensitivity of A172 *IDH1*^{R132H} cells to the GSK-J4 and Belinostat combination could be reversed by pretreatment with GSK864 (**Figure 3G).** Similarly, drug sensitivity of MGG152 cells could be partly recovered after long-term passaging with GSK864 (**Figure S3F**). Together, these results indicate that the combined treatment of GSK-J4 and Belinostat is selectively potent against *IDH1*-mutant glioma cells.

GSK-J4 and Belinostat combination leads to apoptosis in *IDH1*-mutant glioma cells

To address the mechanism behind the reduction in cell viability upon treatment, we first investigated the cell cycle profile of glioma cells. A notable difference in cell cycle progression was observed upon Belinostat treatment, where flow cytometric measurements showed that Belinostat caused a G2/M arrest in both the primary MGG152 cells as well as A172 *IDH1*^{R132H} cells (**Figure S4B**). We then investigated caspase activity of glioma cells. While GSK-J4 or Belinostat as single agents only slightly increased Casp3/7 activity, combinatorial treatment resulted in significant elevation of Casp3/7 activity in A172 *IDH1*^{R132H} cells (**Figure 3H**). Cleavage of poly (ADP-ribose) polymerase-1 (PARP-1), an important hallmark of apoptosis, was also enhanced upon combinatorial treatment in A172 *IDH1*^{R132H} cells, but not in A172 wild-type cells (**Figure 3I**). PARP-1 and Bid cleavage was also observed in MGG152 primary cells upon combination treatment (**Figure S4F).** Application of the general caspase inhibitor Z-VAD-FMK prevented the GSK-J4 and Belinostat induced reduction in cell viability (**Figure 3J).** A fluorescence dye-based "live/dead assay" utilizing YO-PRO-1 staining, demonstrated a significant number of apoptotic cells upon combinatorial treatment in A172 *IDH1*^{R132H} cells (**Figure S4C).** To investigate the changes in the apoptotic program in glioma cells, we examined the expression levels of anti-apoptotic proteins Bcl-XL and XIAP (**Figure S4D, S4E)**. Accordingly, Belinostat decreased XIAP expression levels in all cells tested, and the Bcl-xL levels in the *IDH1*-mutant cells (**Figure S4D, S4E**). Indeed, overexpression of Bcl-XL partly recovered the GSK-J4 and Belinostat induced cell death in A172 *IDH1*^{R132H} cells and primary MGG152 cells (**Figure S4F, S4G**). Taken together, these results indicate that the GSK-J4 and Belinostat induced reduction in cell viability involves the activation of apoptotic programs in *IDH1*-mutant cells.

RNA-seq analysis on 1º *IDH1*-mutant glioma cells reveals global changes and stress response activation upon GSK-J4 and Belinostat treatment.

To assess the mechanism behind GSK-J4 and Belinostat induced cell death in *IDH1*-mutant cells, we performed global transcriptomic analysis in MGG152 cells upon treatment with compounds individually or in combination over a 2-day treatment window (**Figure 4A).** Principal component analysis (PCA) showed distinct clustering of samples from each condition (**Figure S5A**). While individual treatments caused

significant alterations in the transcriptomes, the greatest changes were observed with the combination treatment (**Figure S5B, S5C**). qRT-PCR analysis validated the differential regulation of selected genes upon individual or combined GSK-J4 and Belinostat treatment of MGG152 cells (**Figure S5D**). GSEA analysis indicated hallmark pathways deregulated with each treatment (**Figure 4B**). The Reactome analysis also demonstrated distinct or common pathways between GSK-J4 and Belinostat individual treatments (**Figure 4C).** The commonly altered networks included activation of "Epithelial-mesenchymal transition", "TNFa signaling by NFkB", "Hypoxia", "Xenobiotic metabolism", and "UV-response-dn"; and inhibition of "Myc targets, E2F targets", and "G2M checkpoint". Major downstream changes observed exclusively upon GSK-J4 included "Activation of genes by ATF4" and "Unfolded Protein Response". Given the numerous cell stress-related pathways observed, we further focused on characterizing the stress-response as an underlying candidate mechanism for selective vulnerability of *IDH1*-mutant cells for GSK-J4 and Belinostat.

Given that ATF4 is a major transcription factor that upregulates survival pathways under stress conditions, or apoptotic pathways under severe stress[20], we first examined the changes in ATF4 signaling in IDH1-mutant cells treated with GSK-J4 and/or Belinostat. We observed ATF4 upregulation in both mRNA (**Figure 4D**) and protein level (**Figure 4F**) upon GSK-J4 treatment. Expression of known ATF4 targets such as *ASNS, DDIT4*, *PSAT1, ATF5 and DDIT3* was also increased upon GSK-J4 treatment (**Figure 4D**). The ATF4 signaling components were majorly affected by GSK-J4, but not by Belinostat treatment. In contrast, the effects of Belinostat were pronounced on anti-apoptotic and cell-cycle related gene expression. Specifically, expression of anti-apoptotic genes, such as *BCL2L1*/Bcl-XL and *BIRC5*/Survivin was decreased, and the major cell cycle regulator *CDKN1A*/p21 was increased upon Belinostat treatment (**Figure 4E).** Interestingly, Belinostat also downregulated the *ATF5* gene, which is known to be responsible for survival under stress conditions[21] (**Figure 4D**). An increase in p21 protein levels was also evident upon Belinostat treatment (**Figure 4F**). Combination treatment induced the pro-apoptotic gene expressions, such as of *PUMA* and *NOXA* (**Figure 4E**). Moreover, use of the SUnSET assay[22] indicated a significant decrease in global translation rate in primary cells upon GSK-J4 treatment either individually or in combination (**Figure 4G**). Together, these results suggest that while GSK-J4 activates ATF4-mediated stress response pathways, Belinostat induces cell cycle arrest and inhibits anti-apoptotic pathways, resulting in a combined effect on *IDH1*-mutant glioma cells.

Blocking the stress response protects *IDH1*-mutant cells from GSK-J4 and Belinostat induced death

Based on our finding that the Integrated Stress Response (ISR) is activated in primary *IDH1*-mutant cells following the epigenetic drug treatment, we sought to address the role of ISR in this vulnerability. We applied ISRIB, an inhibitor of ISR, to *IDH1*-mutant cells and observed significant protection of cells from GSK-J4 and Belinostat induced cell death (**Figure 4I**). These observations were extended to A172 *IDH1*^{R132H} cells, where stress response genes were significantly upregulated upon GSK-J4 and Belinostat treatment (**Figure 5A**). These gene expression changes were suppressed in the presence of GSK864

(**Figure 5A**). Similarly, ISRIB treatment partially recovered A172 *IDH1*^{R132H} cells from GSK-J4 and Belinostat induced death (**Figure 5B**). Moreover, *IDH1*^{R132H} cells were significantly more sensitive to treatment with Thapsigargin, an ER stress inducer, compared to wild-type cells, and this effect could be recovered by GSK864 pre-treatment (**Figure 5C**). Given that *DDIT3*/CHOP is responsible for induction of apoptotic pathways under severe stress[23], we investigated its role in GSK-J4 and Belinostat induced apoptosis. We knocked out *DDIT3* gene via CRISPR/Cas9 (**Figure S7A**), which did not affect the overall viability of cells. However, *DDIT3* ablation significantly protected IDH1^{R132H} cells from both the individual effect of GSK-J4 and its combinatorial effect with Belinostat (**Figure 5D**). Expression of *PUMA* and *NOXA* are known to be induced during ER stress[23]. GSK-J4 and Belinostat mediated induction of both genes was significantly inhibited in *DDIT3* knockout cells (**Figure 5E**). Together, these results point to the Integrated Stress Response (ISR) and its effector DDIT3/CHOP as being important mediators of cell death following combined GSK-J4 and Belinostat treatment.

KDM6A and KDM6B inhibition phenocopies the effects observed with GSK-J4 in *IDH1*-mutant cells

To address the effects of GSK-J4 and Belinostat on the changes of major chromatin marks in *IDH1*-mutant cells, we investigated total protein levels of H3K4me3, H3K9me3, H3K27me3 and H3K27ac levels. As expected, H3K27ac level significantly increased upon Belinostat treatment (**Figure S4A**). H3K27me3 methylation, on the other hand, slightly increased upon GSK-J4 treatment at the low doses that were tested (**Figure S4A**).

We further interrogated the chromatin modifying enzyme targets responsible for the observed effects of GSK-J4. GSK-J4 was developed to selectively inhibit KDM6A/UTX and KDM6B/JMJD3, which are H3K27 demethylases[24]. However, it was shown to have activity towards KDM5B and KDM5C as well[25]. We first employed GSK-J5, an inactive form of GSK-J4, and observed no effect on MGG152 (**Figure 6A**) or A172 *IDH1*^{R132H} (**Figure 6B**) cells when applied individually or with Belinostat. KDM5-specific inhibitors, such as KDM5-C70 and KDOAM25a[26,27], or pan 2-OG inhibitor IOX-1, were also largely ineffective on *IDH1*-mutant cells. On the other hand, KDOBA67, a similar chemical to GSK-J4 that inhibits KDM6 enzymes[28], displayed similar efficacy with GSK-J4 either individually or in combination with Belinostat (**Figure 6C and 6D**).

To complement the chemical tool screening, we undertook a genetic approach and targeted *KDM6A* and *KDM6B* genes either individually or combined in A172 wild-type, A172 *IDH1*^{R132H} and MGG152 cells via CRISPR/Cas9 (**Figure S7B and S7C**). Individual knockout of either gene led to a slight inhibition of growth in A172 *IDH1*^{R132H} cells (**Figure 6E**) and double knockout significantly suppressed cell growth in all cell types. However, inhibition effect was most marked in *IDH1*-mutant cells (**Figure 6F**). Proliferation of *KDM6A* and *KDM6B* double knockout cells was further inhibited by Belinostat treatment (**Figure 6G**), similar to GSK-J4 and Belinostat combination treatment. *KDM6A/KDM6B* double knockout cells also displayed an activation of stress response genes in accordance with our observation with GSK-J4 (**Figure 6H**). Together,

these results support that inhibition of KDM6A and KDM6B phenocopies the effects observed with GSK-J4 in *IDH1*-mutant cells.

GSK-J4 and Belinostat combination inhibits intracerebral growth of *IDH1*-mutant glioma *in vivo*

We next tested whether systemic delivery of GSK-J4 and Belinostat to an intracranial xenograft model can demonstrate therapeutic potential. We labeled MGG152 cells with Luciferase, and upon orthotopic injection, monitored tumor formation by non-invasive bioluminescence imaging. When the tumors reached detectable volumes, we administered GSK-J4 and Belinostat or control solutions intraperitoneally for 6 days (**Figure 7A**). GSK-J4 and Belinostat co-treatment significantly decreased tumor volume compared to the control group (**Figure 7B**). Prior to drug treatment, on day 15, average tumor volumes between the animals were comparable, but at the end of treatment period, average tumor volume was significantly lower in the drug-treated group. This difference was maintained until day 28 (**Figure 7C**). Treatment-induced tumor growth inhibition was translated into survival benefit as Kaplan-Meier survival plot indicated significantly longer survival of animals treated with the combination regimen (**Figure 7D**). Taken together, these results demonstrate the combined efficacy of GSK-J4 and Belinostat on orthotopic growth of IDH mutant glioma *in vivo.*

DISCUSSION:

IDH1 mutation is very common in low grade glioma and secondary glioblastoma. The most recent classification of WHO divides each glioma subgroup into *IDH*-wildtype or *IDH*-mutant subtypes[29]. However, there is no treatment specifically designed for *IDH*-mutant glioma. In this study, based on their discrete epigenetic phenotype[5], we interrogated the epigenetic vulnerabilities of *IDH*-mutant gliomas with a chemical screening approach and identified a potent epigenetic drug combination for *IDH1*-mutant glioma cells. Accordingly, GSK-J4 and Belinostat, at doses insufficient to inhibit tumor cell viability as monotherapy, exhibited a powerful synergistic effect on *IDH1*-mutant cells when applied in combination, with minimal effects on *IDH1*-wild-type or non-malignant cells.

To our knowledge, this study is the first to describe an epigenetic targeting screen specifically on *IDH*-mutant cells. In the screen with chemical tools against several chromatin modifiers such as HDACs, HATs, HMTs, KDMs, PHDs, DNMTs, methyl lysine binders, and Bromodomain proteins, we found that 5 compounds demonstrated potent anti-proliferative effects on primary *IDH1*-mutant cells, namely 5-azacytidine, Chaetocin, GSK-J4, Belinostat and TrichostatinA. Among them, only 5-azacytidine was previously shown to be effective against *IDH*-mutant glioma[9]. Indeed, there are ongoing clinical trials for individual 5-azacytidine treatment or combination with mutant IDH inhibitors (Clinical trial identifiers: NCT02677922, NCT03684811).

Our study employed patient-derived primary glioma cells that grow as neurospheres and maintain *IDH1* mutation[18], which are accepted as highly valuable tools to conduct *in vitro* experiments. However, they could not provide sufficient information on the causality between *IDH1* mutation and drug vulnerability. Thus, we established paired cell line models via ectopic overexpression of IDH1^{R132H} in established cell lines that carry wild-type *IDH1*. It is well-known that *IDH1* mutation is found as heterozygous since mutant IDH1 uses α-KG produced by wild-type enzyme as substrate[30]. Therefore, our model was convenient to observe the effects of 2-HG production caused by mutant IDH1. In these complementary *in vitro* models, we observed a clear selective sensitivity of *IDH1^{R132H}* cell lines to GSK-J4 and Belinostat. Given the sensitivity of 2 different primary *IDH1*-mutant cells as well as these established paired models, it is clear that mutant IDH1 induces a vulnerability against GSK-J4 and Belinostat combination treatment.

IDH1 mutation is an early genetic event in tumorigenesis of LGG, and it is conserved in recurrent tumors[6]. Therefore, many inhibitors specific to mutant IDH1 enzyme have been developed as prime clinical candidates[7,8]. In our study, we used the mutant IDH1 inhibitor, GSK864, as a tool to study 2-HG mediated effects of the *IDH1* mutation. We showed that alterations in gene expression signatures caused by the *IDH1* mutation, and selective vulnerability to GSK-J4 and Belinostat, were reversible with GSK864 application. Similarly, induction of cell stress and apoptosis related pathways were also partly reversed by GSK864. These results are in line with previous reports demonstrating the effects of mutant IDH inhibitors[14,15,31]. Our study suggests that the specific phenotypes and resulting vulnerabilities created by *IDH1* mutation may be abrogated by mutant IDH1 inhibitors capable of depleting 2-HG production. Therefore, rather than blocking mutant IDH1 activity in tumors, we postulate that the exploitation of selective vulnerabilities caused by the *IDH1*-mutation might be of significant importance for future clinical translational efforts.

Our findings reveal that the ISR is activated in *IDH1*-mutant cells because of increased cellular stress. This is in accordance with reports showing that 2-HG inhibits oxygen sensors such as prolyl hydroxylase (EGLN, PHD) enzymes and causes ER stress via immature collagen accumulation in brain cells of *Idh1*-R132H knock-in mice[32]. Another study indicated that 2-HG alters TCA cycle and glutamine metabolism and increases mitochondrial stress[11]. Similarly, immune response pathways and genome instability were shown to be upregulated in *IDH*-mutant cells, as a result of activation of endogenous retroviruses (ERVs), which are normally quiescent[33]. ERV activation was also shown to induce ER stress and UPR[34]. Our transcriptomic analyses of paired wild-type and *IDH1^{R132H}* cells revealed similar results, where IFN-α, IFN-γ, inflammatory response pathways and UPR were activated in *IDH1^{R132H}* cells compared to wild-type counterparts. In contrast, these pathways were all downregulated in the presence of GSK864. Therefore, our results suggest that *IDH1*-mutant cells have an increased basal cellular stress, but up to tolerable levels at which the cells can survive. However, GSK-J4 and Belinostat treatment may increase cell stress above this tolerable threshold, leading to subsequent cell death.

We observed a synergy between GSK-J4 and Belinostat, two drugs with distinct effects on gene expression in *IDH1*-mutant cells. While GSK-J4 treatment mainly activated stress response related genes, Belinostat activated cell cycle and apoptosis related genes in *IDH1*-mutant cells. ATF4 is a major transcription factor that upregulates survival pathways under stress conditions, or apoptotic pathways under severe stress. Different stress conditions such as amino acid deprivation, viral infection, ER stress, oxidative stress trigger phosphorylation of eIF2α as a part of ISR[20], suppressing global translation, but inducing specific cap-independent translation of genes such as ATF4. Indeed, GSK-J4 induced *ATF4* as well as its known targets such as *ASNS, DDIT4 and PSAT1*, an effect observed also in the genetic *KDM6A* and *KDM6B* double-knockout model. It was recently shown that inhibition of epigenetic enzymes, including KDMs, may decrease the transcriptional heterogeneity in tumor cells, and sensitize cells to combination with a second agent[35]. While we observed a slight change in global H3K27 methylation levels upon GSK-J4, we observed marked increase in H3K27 acetylation upon Belinostat treatment, in line with our expectations. Therefore, GSK-J4 might be exerting loci-specific actions in *IDH1*-mutant cells, prompting further studies.

The class I HDAC inhibitor Belinostat, increased histone acetylation in *IDH1*-mutant cells. Studies show different mechanisms of action for HDACi, such as upregulation of pro-apoptotic genes, downregulation of anti-apoptotic proteins, induction of ER stress, cell cycle arrest and apoptosis [36,37]. In line with these reports, we observed that expression of anti-apoptotic genes, such as *BCL2L1*/Bcl-XL and *BIRC5*/Survivin, decreased upon Belinostat treatment. Belinostat also led to downregulation of the *ATF5* gene, a known target of ATF4 responsible for survival pathways under stress conditions[21]. Belinostat also caused a G2/M arrest in *IDH1*^{R132H} cells and led to cell death through apoptosis. Interestingly, a clear induction of p21 by Belinostat, which may be responsible for cell cycle arrest, was reduced to basal levels by combination treatment. Besides its growth inhibitory effects, p21 has anti-apoptotic effects and is downregulated by *DDIT3*/CHOP during increased stress conditions[38]. We show that combination treatment increases *DDIT3*/CHOP, which upregulates *PMAIP1*/NOXA and *BBC3*/PUMA and likely downregulates *CDKN1A*/p21. Moreover, we observed significant recovery of GSK-J4 and/or Belinostat effects in *DDIT3* depleted *IDH1*^{R132H} cells. These results indicate that GSK-J4 and Belinostat treatment exacerbates cellular stress, which is already high in *IDH1*-mutant cells, and leads to apoptosis through *DDIT3*/CHOP induction.

Our findings present a model highlighting the effects of GSK-J4 and Belinostat in *IDH1*-mutant glioma cells (**Figure 7D**). We show that mutant IDH1 enzyme leads to activation of cellular stress responses, which facilitate cell survival. Inhibition of KDM6A and KDM6B enzymes through GSK-J4 treatment increases this cellular stress and induces ATF4-mediated ISR. Moreover, inhibition of HDACs with Belinostat downregulates anti-apoptotic proteins and induces cell cycle arrest. Together, they further cause severe stress leading to *DDIT3*/CHOP mediated induction of apoptotic genes and eventually caspase 3/7-mediated apoptosis.

The *in vivo* studies with our patient-derived *IDH1*-mutant animal model support clinical translation of our findings. Only 6-day-treatment of GSK-J4 and Belinostat reduced tumor growth, revealing therapeutic potential of this combination. GSK-J4 was shown to be effective on pediatric brainstem glioma *in vivo*, demonstrating its ability to penetrate the blood-brain barrier (BBB)[39]. It was also reported that Belinostat can cross the BBB and has antitumor effects in an orthotopic rat glioma model[40]. Our results add to the growing evidence and list of epigenetic compounds with ability to target brain tumors. However, GSK-J4 is known to have low stability in physiological conditions, and more stable KDM6 inhibitors will need to be developed for clinical translation. As the frontline therapy for glioblastoma includes use of temozolomide (TMZ), a combination with TMZ might be applicable in a clinical setting. We show that *IDH1*-mutant cells are more sensitive to TMZ as reported[17], and that the effects of drugs, especially Belinostat, are more pronounced in the presence of TMZ (**Figure S6**). In conclusion, our study identifies combined targeting of KDM6A/B and HDACs as a potent and selective therapeutic strategy for the treatment of *IDH1*-mutant glioma.

METHODS:

Reagents: The epigenetic chemical probe library was constructed as described [41]. Bulk amounts of GSK-J4 and Belinostat were purchased from Adooq Bioscience (CA, USA) for *in vivo* experiments. D-2-Hydroxyglutarate (D2HG) Assay Kit was purchased from Sigma-Aldrich (USA). GSK864 was kindly provided by SGC Toronto. Z-VAD-FMK (general caspase inhibitor) and Z-FA-FMK (negative control) were commercially supplied from BD Pharmingen (CA, USA). ISRIB and TMZ were provided by SelleckChem (USA). Anti-IDH1 R132H (Hu) from mouse (clone: H09) antibody was purchased from Dianova (Germany). Anti-PARP, anti-ATF4 (D4B8), anti-p21 (12D1), anti-H3 (D1H2), anti-H3K4me3 (C42D8), anti-H3K9me3 (D4W1U), anti-H3K27me3 (C36B11), and anti-H3K27ac (D5E4), were purchased from Cell Signaling Technology (USA). Anti-GAPDH and anti-α-tubulin were purchased from Abcam (UK). Anti-puromycin (4G11) antibody was purchased from Merck Millipore (USA). GSK-J5, Thapsigargin and Cycloheximide were purchased from Cayman Chemical (USA). D-luciferin was purchased from Biotium (CA, USA).

Cell culture: 293T human embryonic kidney cells (HEK 293T), A172 and LN18 glioblastoma cell lines were purchased from American Type Culture Collection (ATCC, USA). Human astrocytes (HAs) were purchased from ScienCell Research Laboratories (CA, USA). Fibro1 and Fibro2 fibroblast cell lines were established at Koç University School of Medicine from incision biopsies of glioblastoma patients undergoing tumor resection at Koç University Hospital (Ethics approval no: 2013-5). These cells were cultured in DMEM (Gibco, USA), with 10% FBS (Gibco, USA) and 1% Pen/Strep (Gibco, USA) in a 37°C incubator with 5% CO_2. HAs were cultured on Poly-L-Lysine coated plates. MGG119 and MGG152 *IDH1*-mutant cell lines were established with patient-derived xenograft model [18]. They were cultured as neurospheres in GBM/EF medium consisting of neurobasal medium (Gibco, USA) with 7.5 ml L-Glutamine, 1X B-27 supplement

(Gibco, USA), 0.5X N-2 supplement (Gibco, USA), 0.5 ml heparin solution (0.2%, StemCell Technologies, Canada), 0.5% Pen/Strep, FGF (20 ng/ml), EGF (20 ng/ml).

Viral packaging and transduction: Retroviral particles from pMIG Bcl-xL (Addgene plasmid #8790), and lentiviral particles from pLenti6.3/TO/V5 containing *IDH1*^{R132H}[14], or pLentiCRISPRv2 (Addgene #52961) were produced in HEK 293T cells. Briefly, 293T cells were seeded on 10 cm-plates as 2.5x10^6 cells/plate. The next day, with approximately 70-80% confluency, cells in each plate were transfected with required viral plasmids (2500 ng), and packaging plasmids; psPAX2 (2250 ng) or pUMVC (2250 ng), for lentiviral or retroviral packaging, respectively, and VSVG (250 ng) by using 20 µl of FugeneHD (Promega, USA). After overnight incubation, media were refreshed. Virus containing media from 48- and 72-hours post transfection were collected. Then, they were aliquoted either directly or after 100X concentrated with Polyethylene glycol (PEG 8000, Sigma-Aldrich, USA) overnight, and stored at -80^{o}C.

Adherent glioblastoma cells were seeded as 100.000 cells/well of 6-well plate, and transduced next day with virus containing media. Protamine sulfate (PS, 8 µg/ml) was also added to increase transduction efficiency. Primary glioblastoma cells cultured as suspension, were transduced with spinfection method. Briefly, neurospheres were resuspended in 2 mL of EF medium supplemented with PS (8 µg/ml) and seeded on 1 well of 6-well plates together with concentrated virus. Then, cells were centrifuged in a plate-centrifuge (Beckman Coulter, USA) at 800g for 90 minutes. Both adherent and suspension cells were incubated overnight in the cell culture incubator, and then, media were refreshed. 48 hours post-transduction, adherent and suspension cells infected with pLentiCRISPRv2 were treated with 2 µg/ml or 1 µg/ml of puromycin, respectively, and selected for 3 days. A172 cells infected with pLenti6.3/TO/V5 containing *IDH1*^{R132H} were selected with blasticidin (10 µg/ml) for 5-7 days. Efficiency of pMIG BcL-xL infections was monitored via GFP expression under fluorescence microscope.

Chemical screen with epigenetic inhibitors: MGG119 and MGG152 spheres were dissociated into individual cells and seeded in 96-well plates as 4000 cells/well. They were cultured for 24 hours and treated with the chemical probe library consisting of 46 inhibitors targeting bromodomains (BRD), histone deacetylases (HDAC), histone methyltransferases (HMT), lysine demethylases (KDM), prolyl hydroxylases (PHD), methyl lysine binders, DNA methyltransferases (DNMT), poly ADP ribose polymerase (PARP), kinase inhibitors, and histone acetyltransferases (HAT) (**Supplementary Table 1**). Compound effects were compared to cells cultured in the presence of DMSO alone, while media only wells acted as a background control. Cell viabilities were determined via Cell Titer-Glo (CTG) Cell Viability Assay following 48 hours of culture, as described in the section “Cell Viability and Caspase Activity Assays”. All treatments were performed in triplicates.

Validation of screen hits individually or in combination: MGG119, MGG152, Fibro1 and Fibro2 cells were treated with 5-azacytidine, Chaetocin, GSK-J4 and Belinostat, in a dose-dependent manner. Cell viability assays were performed following 72h of treatment. Both tumor and non-malignant cell lines were

subjected to dual combinations of these inhibitors. Human astrocytes (HA) were treated with GSK-J4 (2.5 µM) and Belinostat (1 µM) individually or in combination. Combination index (CI) values which is a measure of drug synergy were calculated using CompuSyn software[42].

Generation of *IDH1*-mutant cell lines: *IDH1*-mutant glioblastoma cell lines were generated by lentiviral infection of pLenti6.3/TO/V5 containing $IDH1^{R132H}$[14]. Cells were cultured in parallel with parental wild-type cells to obtain a paired cell line. The expression of mutant IDH1 was confirmed using western blot and immunocytochemical staining, using $IDH1^{R132H}$ mutant specific antibody (DIA-H09, Dianova, Germany). 2-HG production was assessed using the D-2-Hydroxyglutarate (D2HG) Assay Kit (Sigma-Aldrich, USA) in the presence or absence of GSK864. Paired glioblastoma cell lines were also treated with inhibitors individually and in combination. Cell viabilities were determined after 72h of treatments as described below.

Cell viability and caspase activity assays: Cell viabilities were measured via Cell Titer-Glo (CTG) Luminescent Cell Viability Assay (Promega, USA) according to manufacturer's instructions with some modifications. Briefly, cells were seeded to clear bottom black side 96-well plates (Corning Costar) as 4000 cells/well in triplicates. The next day, they were treated with corresponding chemicals of interest individually or in combination for the defined periods. At the end of the treatment period, media from each well were removed via multi-well pipette. 44 µl of CTG ready-to-use mix, which is prepared as 1:10 dilution of CTG reagent with DMEM, were added on each well. For primary cells cultured as suspension, CTG reagent was directly added on cells at 1:10 amount of culture medium. After 2 minutes of shaking and 8 minutes of incubation, luminescence levels of each well were measured using a plate reader (BioTek's Synergy H1, Winooski, VT, USA). Relative cell viabilities were calculated by using luminescent values of untreated samples as control.

For Caspase 3/7 activity assay, A172 wild-type and $IDH1^{R132H}$ cells were seeded on 96-well plates as 4000 cells/well. The next day, cells were treated with GSK-J4 (2.5 µM) and/or Belinostat (1 µM). After 48h of drug treatments, Caspase 3/7 activities in each well were measured via Caspase Glo 3/7 assay (Promega, USA), according to manufacturer's instructions.

Caspase inhibition, stress response inhibition, and mutant IDH1 inhibition assays: For caspase inhibition assay, Z-FA-FMK (Negative Control for Caspase Inhibitors) or Z-VAD-FMK (General Caspase Inhibitor) pre-treatments were performed at 20 µM final concentration for 24h before following drug treatments. For ISR inhibition, ISRIB (1 µM) pre-treatment was performed, respectively for 24h before drug treatments. For inhibition of mutant IDH1 enzyme, cells were pre-treated with GSK864 (2.5 µM), a selective $IDH1^{R132H}$ inhibitor[8] for 3 days before any assay or drug treatment. Primary MGG119 and MGG152 cells were treated with GSK864 (2.5 µM) for 10 passages to observe long term effects.

Live cell imaging: Olympus Xcellence Pro inverted microscope with 10X air objective (Center Valley, PA, USA) was used for the live-cell imaging experiments in a 37°C chamber supplied with 5% CO_2. A172 wild-type and $IDH1^{R132H}$ cells were seeded on 24-well plates at a density of 16.000 cells/well. Next day, they

were treated with either GSK-J4 (2.5 µM) or Belinostat (1 µM), or in combination. Images of random positions from each well were captured with 8-10 min intervals during 96h after drug treatment. Cell numbers in 3 different frames for each condition was counted using ImageJ software (NIH Image, MD, USA) and viability curves were obtained for each condition.

Co-culture experiments: Fibro1 fibroblasts were infected with GFP-expressing lentiviruses, and A172 *IDH1*^{R132H} cells were infected with mCherry-expressing lentiviruses. Fibroblasts and A172 *IDH1*^{R132H} cells were admixed and seeded on 6-well plates with 1:1 ratio. Co-culture wells were subjected to either no treatment, GSK-J4 alone (2.5 µM), Belinostat alone (1 µM), or their combination. After 72h of drug treatments, fluorescent images were taken under red and green fluorescent filters, and viable cells were quantified by counting 3 different frames for each condition.

Cell cycle analysis: A172 wild-type, A172 *IDH1*^{R132H} and MGG152 cell pellets were collected after 24h or 48h of either without treatment or treatments with GSK-J4, Belinostat and their combination. They were washed with PBS and fixed with 200 µl of cold 70% ethanol via incubating for 30 min at 4^{o}C. Ethanol was added dropwise, and pellets were resuspended either with flicking tube or pipetting gently after each drop. After fixation, cells were centrifuged at 850g for 5 min, and washed 2 times with PBS. To remove RNA content, pellets were resuspended in 50 µl of 100 µg/ml RNase and incubated for 15 min at room temperature. Finally, 200 µl of 50 µg/ml propidium iodide (PI) solution was added on samples, and they were incubated for 30 min at room temperature. Samples were kept in the dark at 4^{o}C until analysis was performed. Quantification of PI staining were performed via flow cytometry (BD Accuri C6 Plus Flow Cytometry, BD Biosciences, USA), and cell cycle intervals were determined by assigning the n peak as G0/G1 phase, n to 2n interval as S phase and 2n peak as G2/M phase.

YO-PRO-1 staining: A172 wild-type and *IDH1*^{R132H} cells were seeded on 24-well plates as 20.000 cells/well. Next day, cells were either kept untreated or treated with GSK-J4 (2.5 µM) and Belinostat (1 µM) in combination. After 48h of drug treatments, media were removed, and cells were kept in fresh media containing 0.1% (v/v) YO-PRO-1 stock solution. Plates were incubated at 37^{o}C for 15 min, and fluorescent images were taken directly, as soon as possible upon incubation.

Western blotting and SUnSET assay: Cell pellets were collected after 24h or 48h of indicated drug treatments and stored at -80^{o}C. Pellets were lysed in NP40 lysis buffer (1% NP40, 50 mM Tris buffer pH 7.4, 250 mM NaCl, 5mM EDTA, 50 mM NaF, 0.02% NaN_3) supplemented with 1X protease inhibitor cocktail set (cOmplete™ ULTRA Tablets, Roche, Germany) and 1mM PMSF prior to usage. Cell lysates were centrifuged at 13.000 rpm for 10 min at 4^{o}C, and supernatants were collected. For histone analysis, pellets were lysed in Triton Extraction Buffer (TEB) which consists of PBS with 0.5% Triton X 100 (v/v), 2 mM PMSF, 0.02% (w/v) NaN3 and 5 mM sodium butyrate, on ice for 10 min. Nuclei were precipitated via centrifugation at 6500 g for 10 min at 4^{o}C, and washed again with TEB after discarding supernatants. Pellets were resuspended in 0.2N HCl as around 10^7 cells/ml and kept at 4^{o}C overnight. Next day, lysates were

neutralized by adding 1M of NaOH as 1/5 volume of HCl solution. They were centrifuged at 6500 g for 10 min at 4 ºC, and supernatants were stored as histone lysates at -20ºC.

For SUnSET assay[22], MGG152 cells were treated with GSK-J4 and/or Belinostat for 24h or 48h. Thapsigargin (5 µM) or Cycloheximide (5 µM) were used as control treatments. Then, cells were treated with puromycin (10 µM) for 30 min, pellets were collected and lysed in NP40 buffer as explained above.

Protein concentration of lysates from all protocols were determined via Pierce's BCA protein assay kit (Thermo Fisher Scientific, USA). Lysates were mixed with 4X loading dye which is prepared by mixing 4X Laemmli Sample Buffer (Bio-Rad, USA) with 2-mercaptoethanol in 9:1 ratio, and boiled at 95ºC for 10 min. Appropriate amount of samples and protein ladder (Precision Plus Protein, Bio-Rad, USA) were loaded into gradient SDS polyacrylamide gels (Mini-PROTEAN® TGX™ Precast Gels, Bio-Rad, USA), and run at 25 mA for 40 min. Then, protein transfer was performed via Trans-Blot® Turbo™ RTA Mini PVDF Transfer Kit (Bio-Rad, USA) with manufacturer's protocol. Membrane was blocked with 5% non-fat dry milk for 1h with gentle shaking at room temperature. Then, blocking buffer was replaced with primary antibody diluted in PBST with 2% BSA and 0.02% NaN_3 by gently shaking overnight at 4ºC. Next day, antibody solution was removed, and membrane was washed 3 times with PBST for 15 min each. Then, it was incubated with secondary antibody diluted in 5% milk solution for 1h at RT and washed 3 times with PBST for 15 min each. Membrane was incubated with Pierce™ ECL Western Blotting Substrate (Thermo Fisher Scientific, USA) for 5 min at dark, and visualized by Odyssey ® Fc Imaging System (LI-COR Biosciences, USA).

RNA sequencing: A172 wild-type and A172 *IDH1*^{R132H} cells were cultured in the presence or absence of GSK864 (2.5 µM) for 3 days and cell pellets were collected for RNA sequencing. As the second set of samples, MGG152 patient derived *IDH1*-mutant cells were cultured without drugs as control, with GSK-J4 alone, Belinostat alone or with their combination. Cell pellets were collected after 48h of drug treatments. All samples were studied as duplicate.

Total RNAs were extracted with Nucleospin RNA kit (Macherey-Nagel, Germany), according to manufacturer's protocol, and stored at -80 ºC prior to generating RNA-seq libraries. Libraries were prepared using NEBNext Ultra Directional RNA library prep kit for Illumina (NEB, USA), according to manufacturer's instructions. Libraries were then paired-end sequenced using a NextSeq 500 (Illumina) with a read length of 42 bp. Reads were quality controlled using FastQC (version 0.11.4)[43], aligned using HISAT2 (version 2.1.0) [44], and assigned to annotated features using featureCounts (part of the subreads package, version 1.5.0-p2). The Fasta and GTF files for the human genome were obtained from the Ensembl FTP site release 75. Computational pipelines were used by calling scripts from the CGAT toolkit to analyze the next generation sequencing data (https://github.com/cgat-developers)[45,46]. Data have been deposited in NCBI's Gene Expression Omnibus (accession number of GSE134120). Differentially expressed genes (DEGs) were identified using DESeq2[47]. Analysis of enriched pathways were performed using Gene Set Enrichment Analysis (GSEA) and eXploring Genomic Relations (XGR) softwares[19,48]. R scripts used for transcriptomic data analysis are available through github (https://github.com/Acribbs/deseq2_report).

Quantiative RT-PCR: Cell pellets were collected after specified treatments and stored at -80ºC. Total RNAs were isolated via Nucleospin RNA kit (Macherey-Nagel, Germany), according to manufacturer's instructions, and RNA was stored at -80ºC until required. For cDNA production, 1000 ng of total RNA was melted at 65ºC for 5 minutes in the presence of random hexamer, dNTP, and nuclease-free water. Then, samples were incubated at room temperature for 10 minutes in the presence of 5X First Strand (FS) buffer, DTT and RNasin. Finally, reverse transcription was performed using M-MLV RT enzyme in the following conditions: 37ºC for 1 hour, 70ºC for 15 minutes. qRT-PCR was performed by using SYBR green mix (Roche, Switzerland), and Lightcycler 480 instrument (Roche, Switzerland). Relative gene expressions were calculated by using ΔΔCt method, and GAPDH as reference gene. Primers used in qRT-PCR experiments were given in **Supplementary Table 2**.

CRISPR/Cas9 mediated knock-out experiments: gRNA sequences targeting exon regions of KDM6A and KDM6B genes were obtained from GeCKO library designed by Feng Zhang's laboratory at Broad Institute [49]. gRNAs targeting DDIT3 gene were designed using Chopchop gRNA design tool[50]. All gRNAs (**Supplementary Table 3)** were supplied by Macrogen Europe Laboratories as top and bottom strands and they were annealed and cloned into lentiCRISPR v2 plasmid (Addgene #52961) as described[49]. 3 gRNAs targeting each gene were pooled and lentiviruses were produced from these pools for each gene. 2 non targeting gRNAs were pooled and used as control gRNAs (gNT) in further experiments. Cells were infected with MOI of ~3. Then, growth analysis, viability assays after drug treatments and gene expression analysis were performed. Gene knockouts were validated via Sanger sequencing of targeted regions (**Figure S7**).

***In vivo* experiments:** Non-obese diabetic/severe combined immunodeficiency (NOD/SCID) mice were used for generation of orthotopic tumor models. All experiments were performed in Koç University Animal Facility with appropriate conditions and all protocols were approved by the Koç University Ethics Committee. *IDH1*-mutant primary MGG152 cells were infected with lentiviruses containing both Firefly Luciferase and mCherry. 2x10^5 cells were injected intracranially using stereotaxic injection in 7 ul PBS as described[51]. To monitor tumor formation and progression, D-Luciferin (50 mg/kg) was injected intraperitoneally and luminescence due to luciferase activity was measured via in vivo bioluminescence imaging system (IVIS Lumina III). After 17 days of tumor injection, mice were treated with either DMSO or GSK-J4 and Belinostat combination. Both drugs were injected intraperitoneally as 100 mg/kg, for 6 consecutive days. Tumor sizes were calculated as average radiance via Living Image software (PerkinElmer, USA). Kaplan-Meier survival plot was also generated via using GraphPad Prism version 8.0.2 for Windows, GraphPad Software, (CA, USA).

Statistical analysis: All charts were plotted using GraphPad Prism version 8.0 or Microsoft Excel 365 softwares. Two-way ANOVA analyses were performed in GraphPad Prism, and unpaired t-tests were performed in Microsoft Excel using pre-built functions. Combination indexes (CI) were calculated using

CompuSyn software. Gene set enrichment scores, false discovery rate (FDR) values and p-values for enrichment analysis were calculated using GSEA version 4.0 software.

ACKNOWLEDGMENTS:

Financial support was obtained from The Scientific and Technological Research Council of Turkey (TUBITAK) BIDEB Program (#2211e) (AK) and Koç University School of Medicine. Funding for this project was also received from Bone Cancer Research Trust (AC, UO), Rosetrees Trust (UO), CRUK (A23900, UO), the LEAN program grant of the Leducq Foundation (UO), the Oxford NIHR Biomedical Research Centre (UO), and the People Programme (Marie Curie Actions) of the European Union's Seventh Framework Programme (FP7/2007-2013) (UO) under REA grant agreement n° [609305]. The authors acknowledge use of the services and facilities of the Koç University Research Center for Translational Medicine (KUTTAM), funded by the Presidency of Turkey, Presidency of Strategy and Budget.

AUTHOR CONTRIBUTIONS:

Study design: TBO, AK and UO; data generation: AK, GNS, FS, AC, BI, and SA; data analysis: AK, AC, and TBO; data interpretation: TBO, AK, AC, DPC, IS, HW and UO; supplied reagents and lines: DPC, IS, HW and UO; initial manuscript draft: AK and TBO; approved final manuscript: all authors.

COMPETING INTERESTS:

The authors declare no competing interests.

REFERENCES:

1. Gilbert, M. R. *et al.* A randomized trial of bevacizumab for newly diagnosed glioblastoma. *N. Engl. J. Med.* **370**, 699–708 (2014).
2. Parsons, D. W. *et al.* An integrated genomic analysis of human glioblastoma multiforme. *Science (80-.).* **321**, 1807–1812 (2008).
3. Yan, H. *et al.* IDH1 and IDH2 Mutations in Gliomas. *N. Engl. J. Med.* **360**, 765–773 (2009).
4. Ye, D., Xiong, Y. & Guan, K. L. The mechanisms of IDH mutations in tumorigenesis. *Cell Res.* **22**, 1102–1104 (2012).
5. Turcan, S. *et al.* IDH1 mutation is sufficient to establish the glioma hypermethylator phenotype. *Nature* **483**, 479–483 (2012).
6. Watanabe, T., Nobusawa, S., Kleihues, P. & Ohgaki, H. IDH1 mutations are early events in the development of astrocytomas and oligodendrogliomas. *Am. J. Pathol.* **174**, 1149–1153 (2009).
7. Rohle, D. *et al.* An inhibitor of mutant IDH1 delays growth and promotes differentiation of glioma cells. *Science (80-.).* **340**, 626–630 (2013).
8. Okoye-Okafor, U. C. *et al.* New IDH1 mutant inhibitors for treatment of acute myeloid leukemia. *Nat. Chem. Biol.* **11**, 878–886 (2015).
9. Borodovsky, A. *et al.* 5-azacytidine reduces methylation, promotes differentiation and induces tumor regression in a patient-derived IDH1 mutant glioma xenograft. *Oncotarget* **4**, (2013).
10. Turcan, S. *et al.* Efficient induction of differentiation and growth inhibition in IDH1 mutant glioma cells by the DNMT Inhibitor Decitabine. *Oncotarget* **4**, 1729–1736 (2013).

11. Grassian, A. R. *et al.* IDH1 mutations alter citric acid cycle metabolism and increase dependence on oxidative mitochondrial metabolism. *Cancer Res.* **74**, 3317–3331 (2014).
12. Fu, X. *et al.* 2-hydroxyglutarate inhibits ATP synthase and mTOR Signaling. *Cell Metab.* **22**, 508–515 (2015).
13. Sulkowski, P. L. *et al. Oncometabolites suppress DNA repair by disrupting local chromatin signalling*. *Nature* vol. 582 (Springer US, 2020).
14. Tateishi, K. *et al.* Extreme Vulnerability of IDH1 Mutant Cancers to NAD+ Depletion. *Cancer Cell* **28**, 773–784 (2015).
15. Zhang, Y. *et al.* Mutant IDH sensitizes gliomas to endoplasmic reticulum stress and triggers apoptosis via miR-183-mediated inhibition of semaphorin 3E. *Cancer Res.* **79**, 4994–5007 (2019).
16. Wang, Y. *et al.* Targeting therapeutic vulnerabilities with PARP inhibition and radiation in IDH-mutant gliomas and cholangiocarcinomas. *Sci. Adv.* **6**, 1–14 (2020).
17. Lu, Y. *et al.* Chemosensitivity of IDH1-mutated gliomas due to an impairment in PARP1-mediated DNA repair. *Cancer Res.* **77**, 1709–1718 (2017).
18. Wakimoto, H. *et al.* Targetable Signaling Pathway Mutations Are Associated with Malignant Phenotype in IDH-Mutant Gliomas. *Clin. Cancer Res.* **20**, 2898–2909 (2014).
19. Subramanian, A. *et al.* Gene set enrichment analysis: A knowledge-based approach for interpreting genome-wide expression profiles. *Proc. Natl. Acad. Sci. U. S. A.* **102**, 15545–15550 (2005).
20. Pakos-Zebrucka, K. *et al.* The integrated stress response. *EMBO Rep.* **17**, 1374–1395 (2016).
21. Rozo, A. V. *et al.* ATF5 regulates β-cell survival during stress. *Proc. Natl. Acad. Sci.* **114**, 1341–1346 (2017).
22. Schmidt, E. K., Clavarino, G., Ceppi, M. & Pierre, P. SUnSET, a nonradioactive method to monitor protein synthesis. *Nat. Methods* **6**, 275–277 (2009).
23. Li, J., Lee, B. & Lee, A. S. Endoplasmic Reticulum Stress-induced Apoptosis. *J. Biol. Chem.* **281**, 7260–7270 (2006).
24. Kruidenier, L. *et al.* A selective jumonji H3K27 demethylase inhibitor modulates the proinflammatory macrophage response. *Nature* **488**, 404–408 (2012).
25. Heinemann, B. *et al.* Inhibition of demethylases by GSK-J1/J4. *Nature* **514**, E1–E2 (2014).
26. Horton, J. R. *et al.* Structural basis for KDM5A histone lysine demethylase inhibition by diverse compounds The KDM5/JARID1 family of Fe(II)-and α-ketoglutarate-dependent demethylases removes methyl groups from methylated lysine 4 of histone H3. Accumulating evidence supports . *Cell Chem Biol* **23**, 769–781 (2016).
27. Tumber, A. *et al.* Potent and Selective KDM5 Inhibitor Stops Cellular Demethylation of H3K4me3 at Transcription Start Sites and Proliferation of MM1S Myeloma Cells. *Cell Chem. Biol.* **24**, 371–380 (2017).
28. Cottone, L. *et al.* Epigenetic inactivation of oncogenic brachyury (TBXT) by H3K27 histone demethylase controls chordoma cell survival. *bioRxiv* **44**, 432005 (2018).
29. Louis, D. N. *et al.* The 2016 World Health Organization Classification of Tumors of the Central Nervous System: a summary. *Acta Neuropathol.* **131**, 803–820 (2016).
30. Xu, W. *et al.* Oncometabolite 2-hydroxyglutarate is a competitive inhibitor of α-ketoglutarate-dependent dioxygenases. *Cancer Cell* **19**, 17–30 (2011).
31. Nagashima, H. *et al.* Poly(ADP-ribose) glycohydrolase inhibition sequesters NAD+ to potentiate the metabolic lethality of alkylating chemotherapy in IDH mutant tumor cells. *Cancer Discov.* **165962**, CD-20-0226 (2020).
32. Sasaki, M. *et al.* D-2-hydroxyglutarate produced by mutant Idh1 perturbs collagen maturation and basement membrane function. *Genes Dev.* **26**, 2038–2049 (2012).
33. Turcan, S. *et al.* Mutant-IDH1-dependent chromatin state reprogramming, reversibility, and persistence. *Nat. Genet.* **50**, 62–72 (2018).
34. Pasquarella, A. *et al.* Retrotransposon derepression leads to activation of the unfolded protein response and apoptosis in pro-B cells. *Development* **143**, 1788–1799 (2016).
35. Hinohara, K. *et al.* KDM5 Histone Demethylase Activity Links Cellular Transcriptomic Heterogeneity to Therapeutic Resistance. *Cancer Cell* **34**, 939-953.e9 (2018).
36. Havas, A. P. *et al.* Belinostat and vincristine demonstrate mutually synergistic cytotoxicity associated with mitotic arrest and inhibition of polyploidy in a preclinical model of aggressive diffuse large B cell lymphoma. *Cancer Biol. Ther.* **17**, 1240–1252 (2016).

37. Kahali, S., Sarcar, B., Prabhu, A., Seto, E. & Chinnaiyan, P. Class I histone deacetylases localize to the endoplasmic reticulum and modulate the unfolded protein response. *FASEB J.* **26**, 2437–2445 (2012).
38. Mihailidou, C., Papazian, I., Papavassiliou, A. G. & Kiaris, H. CHOP-dependent Regulation of p21/waf1 During ER Stress. *Cell. Physiol. Biochem.* **25**, 761–766 (2010).
39. Hashizume, R. *et al.* Pharmacologic inhibition of histone demethylation as a therapy for pediatric brainstem glioma. *Nat. Med.* **20**, 1394–1396 (2014).
40. Gurbani, S. S. *et al.* Assessing Treatment Response of Glioblastoma to an HDAC Inhibitor Using Whole-Brain Spectroscopic MRI. **5**, 53–60 (2019).
41. Cribbs, A. *et al.* Inhibition of histone H3K27 demethylases selectively modulates inflammatory phenotypes of natural killer cells. *J. Biol. Chem.* **293**, 2422–2437 (2018).
42. Chou, T.-C. & Martin, N. CompuSyn for Drug Combinations and for General Dose-Effect Analysis. **2005**, 3–4 (2010).
43. Wingett, S. W. & Andrews, S. FastQ Screen: A tool for multi-genome mapping and quality control. *F1000Research* **7**, 1338 (2018).
44. Kim, D., Paggi, J. M., Park, C., Bennett, C. & Salzberg, S. L. Graph-based genome alignment and genotyping with HISAT2 and HISAT-genotype. *Nat. Biotechnol.* **37**, 907–915 (2019).
45. Sims, D. *et al.* CGAT: Computational genomics analysis toolkit. *Bioinformatics* **30**, 1290–1291 (2014).
46. Cribbs, A. P. *et al.* CGAT-core: a python framework for building scalable, reproducible computational biology workflows. *F1000Research* **8**, 377 (2019).
47. Love, M. I., Huber, W. & Anders, S. Moderated estimation of fold change and dispersion for RNA-seq data with DESeq2. *Genome Biol.* **15**, 1–21 (2014).
48. Fang, H., Knezevic, B., Burnham, K. L. & Knight, J. C. XGR software for enhanced interpretation of genomic summary data, illustrated by application to immunological traits. *Genome Med.* **8**, 1–20 (2016).
49. Sanjana, N. E., Shalem, O. & Zhang, F. Improved vectors and genome-wide libraries for CRISPR screening. *Nat. Methods* **11**, 783–784 (2014).
50. Labun, K. *et al.* CHOPCHOP v3: expanding the CRISPR web toolbox beyond genome editing. *Nucleic Acids Res.* **47**, W171–W174 (2019).
51. Bagci-Onder, T., Wakimoto, H., Anderegg, M., Cameron, C. & Shah, K. A dual PI3K/mTOR inhibitor, PI-103, cooperates with stem cell-delivered TRAIL in experimental glioma models. *Cancer Res.* **71**, 154–163 (2011).

FIGURES:

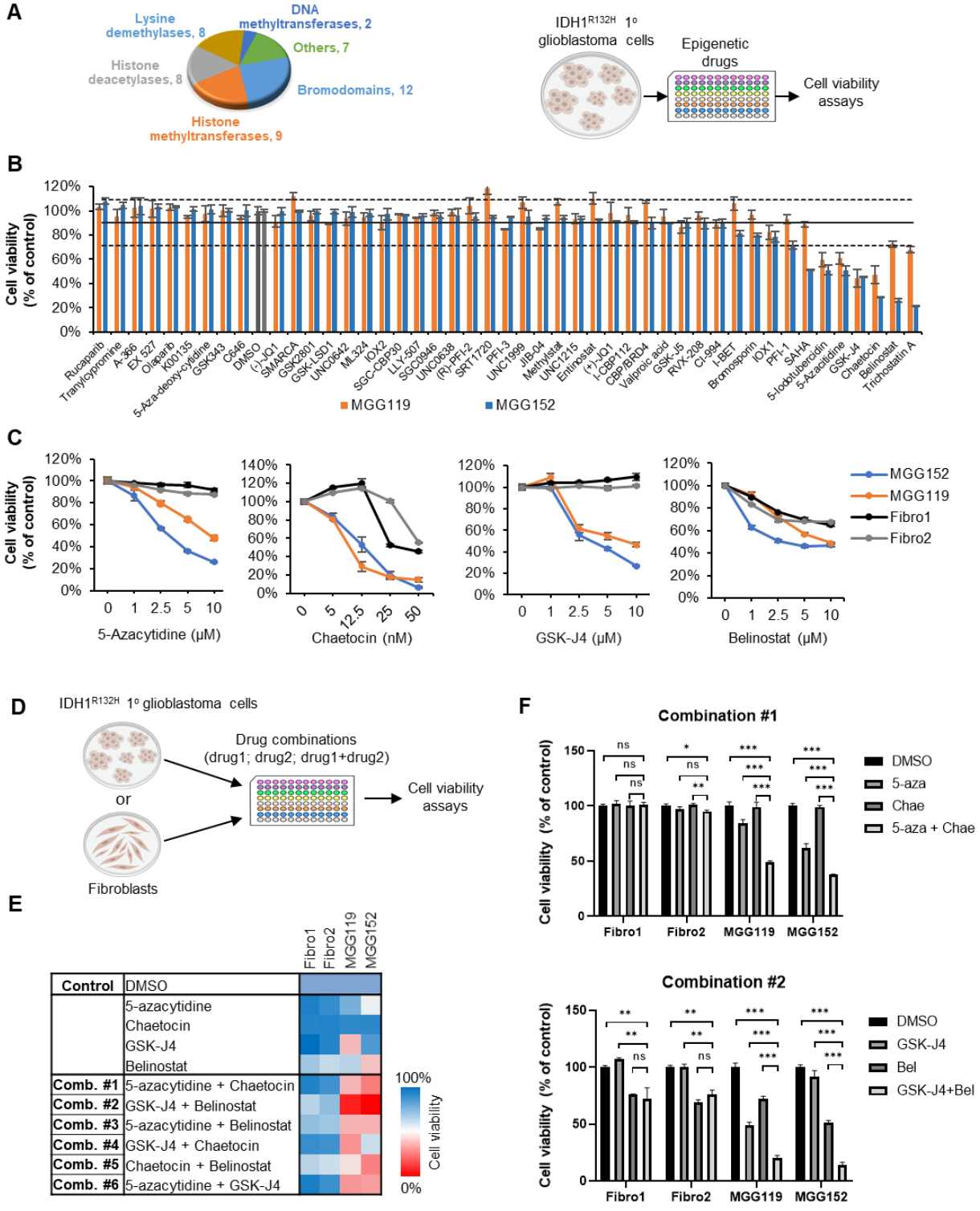

Figure 1. An epigenetic inhibitor screen identifies potential chromatin targets for *IDH1*-mutant gliomas. A) Pie chart shows total of 46 chemical probes targeting different classes of epigenetic enzymes. A compound screen was performed in 96-well plates in triplicate. **B)** Patient derived *IDH1*-mutant MGG119 and MGG152 cells were treated with chemical probe library for 48h. Black and gray bars represents DMSO control. Horizontal black line represents viability mean, staggered lines denote SD=1. **C)** Patient derived *IDH1*-mutant glioblastoma cells and non-malignant fibroblasts were treated with screen hits individually at increasing doses for 72h; the tumor cells were markedly more sensitive to drug treatment. **D)** Schematic view of compound combination strategy for *IDH1*-mutant primary glioblastoma cells and patient-derived fibroblasts. **E)** Glioblastoma cells and fibroblasts were treated with all possible dual combinations of screen hits. Effects of individual and combinatorial treatments on viability are represented as heat map. Color scale indicates viability, increasing from red to blue. **F)** Combination of 5-azacytidine (2.5 µM) and Chaetocin (5 nM), or GSK-J4 (2.5 µM) and Belinostat (1 µM) are potent epigenetic drug combinations for *IDH1*-mutant gliomas. p-values were determined by unpaired t test; ns, non-significant; *$p < 0.05$; **$p < 0.01$; ***$p < 0.001$.

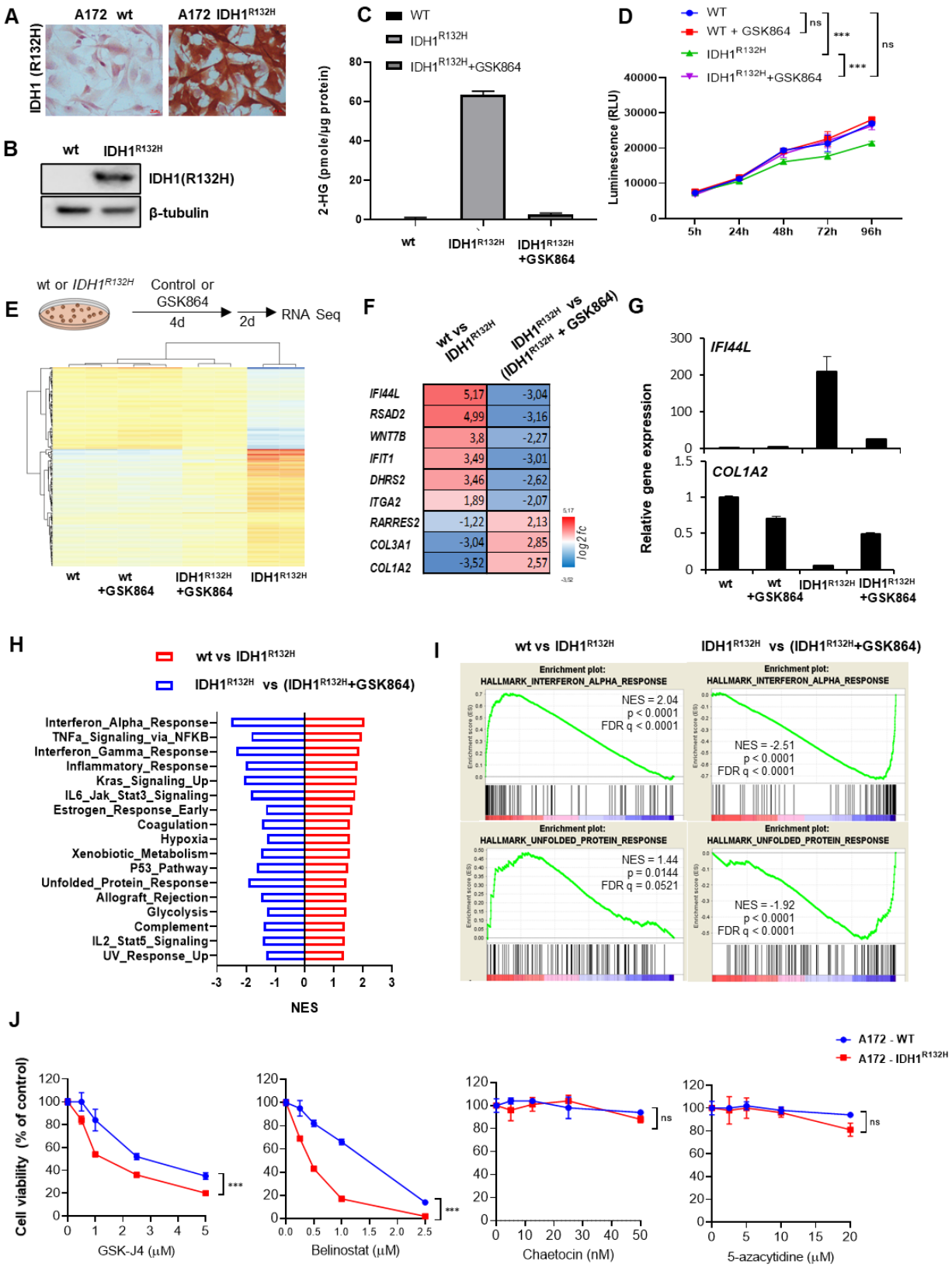

Figure 2. IDH1^{R132H} overexpression leads to global transcriptome alterations that are reversible with GSK864, an inhibitor of IDH1^{R132H}. Mutant IDH1 enzyme (IDH1^{R132H}) was overexpressed in A172 cells to generate wild-type and mutant cell pairs. Overexpression was validated via immunohistochemical staining **(A)** and western blot **(B)** using anti-IDH1 (R132H) antibody. **C)** The level of 2-HG was highly increased via IDH1^{R132H} overexpression, and blocked with GSK864 (2.5 μM), an inhibitor of mutant IDH1 enzyme. **D)** IDH1^{R132H} overexpression slowed down the growth of A172 cells, and this was recovered with GSK864. **E)** Heatmap of differentially expressed genes (DEGs) between A172 wild-type and *IDH1^{R132H}* cells with or without GSK864. All DEGs upregulated in *IDH1^{R132H}* cells were downregulated with GSK864, and vice versa. **F)** The log2 fold changes of highest ranking DEGs in RNA-seq analysis of wild-type and *IDH1^{R132H}* samples. **G)** Validation of RNA-seq results via qRT-PCR using selected genes *IFI44L* and *COL1A2*. **H)** GSEA results showing hallmark pathways changing upon IDH1^{R132H} overexpression. All pathways upregulated in *IDH1^{R132H}* cells were downregulated with GSK864. NES, normalized enrichment score. **I)** Interferon alpha response and unfolded protein response pathways were significantly activated in *IDH1^{R132H}* cells and inhibited with GSK864. FDR, false discovery rate. **J)** A172 wild-type and *IDH1^{R132H}* cells were treated with screen hits individually at different doses for 72h. *IDH1^{R132H}* cells were more sensitive to GSK-J4 and Belinostat than wild-type cells. For panel D and J, p-values were determined by 2-way ANOVA; ns, non-significant; *$p < 0.05$; **$p < 0.01$; ***$p < 0.001$.

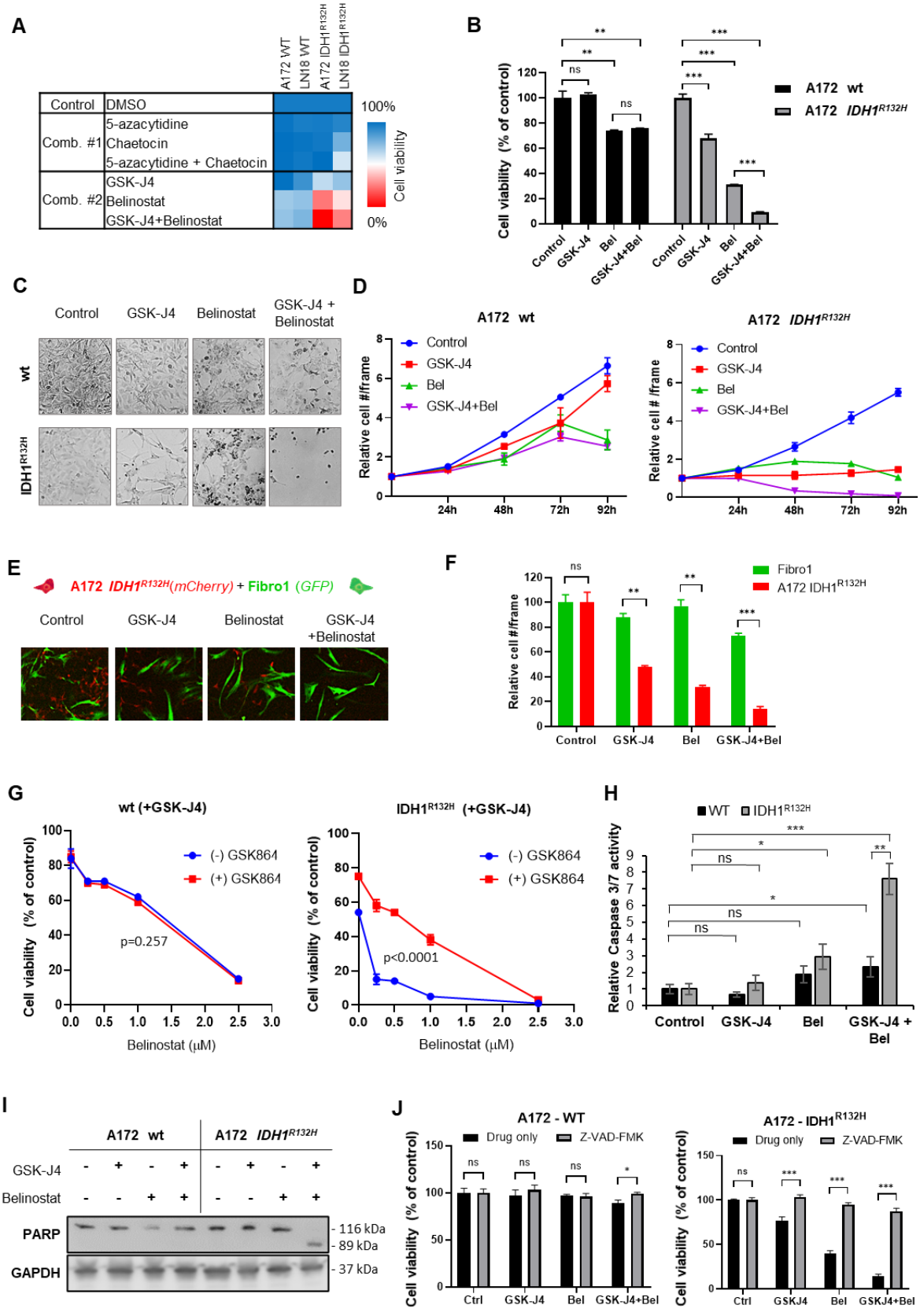

Figure 3. GSK-J4 and Belinostat combination selectively targets *IDH1^{R132H}* glioma cells *in vitro*. A) Heatmap of the effect of compound combinations on viability of A172 and LN18 wild-type and *IDH1^{R132H}* cell pairs. **B)** The GSK-J4 and Belinostat combination was highly effective on A172 *IDH1^{R132H}* cells, while it did not cause an additional effect on wild-type cells. **C)** Live cell images of A172 wild-type and *IDH1^{R132H}* cells after 96h of control, GSK-J4 (2.5 µM), Belinostat (1 µM) or GSK-J4 + Belinostat treatments. **D)** Quantification of live cell images indicate that *IDH1^{R132H}* cells were completely eliminated with GSK-J4 + Belinostat combination, while few cells were dead in wild-type cells. **E)** mCherry-labelled A172 *IDH1^{R132H}* cells were co-cultured with GFP-labelled fibroblasts and treated with GSK-J4 and Belinostat individually and in combination. **F)** Quantification of co-culture images indicated that fibroblasts were not markedly affected by either GSK-J4, Belinostat or combination. However, A172 *IDH1^{R132H}* cells diminished after individual or combination treatments. **G)** GSK864 (2.5 µM) pre-treatment recovered sensitivity of A172 *IDH1^{R132H}* cells against GSK-J4 and Belinostat treatments, while it has no effect on wild-type A172 cells. Horizontal axis represents increasing concentration of Belinostat in the presence of 2.5 µM of GSK-J4. **H)** Caspase-Glo 3/7 activity assay showed that GSK-J4 and Belinostat combination treatment highly increased the Caspase 3/7 activity of A172 *IDH1^{R132H}* cells, compared to wild-type cells. **I)** PARP cleavage was pronounced in Western blots of A172 *IDH1^{R132H}* cells upon GSK-J4 and Belinostat co-treatment. **J)** Z-VAD-FMK, a general caspase inhibitor, recovered the effects of GSK-J4 and Belinostat treatments on the viability of A172 *IDH1^{R132H}* cells. For panel G, p-values were determined by 2-way ANOVA, for all other panels, p-values were determined by unpaired t test; ns, non-significant; *$p < 0.05$; **$p < 0.01$; ***$p < 0.001$.

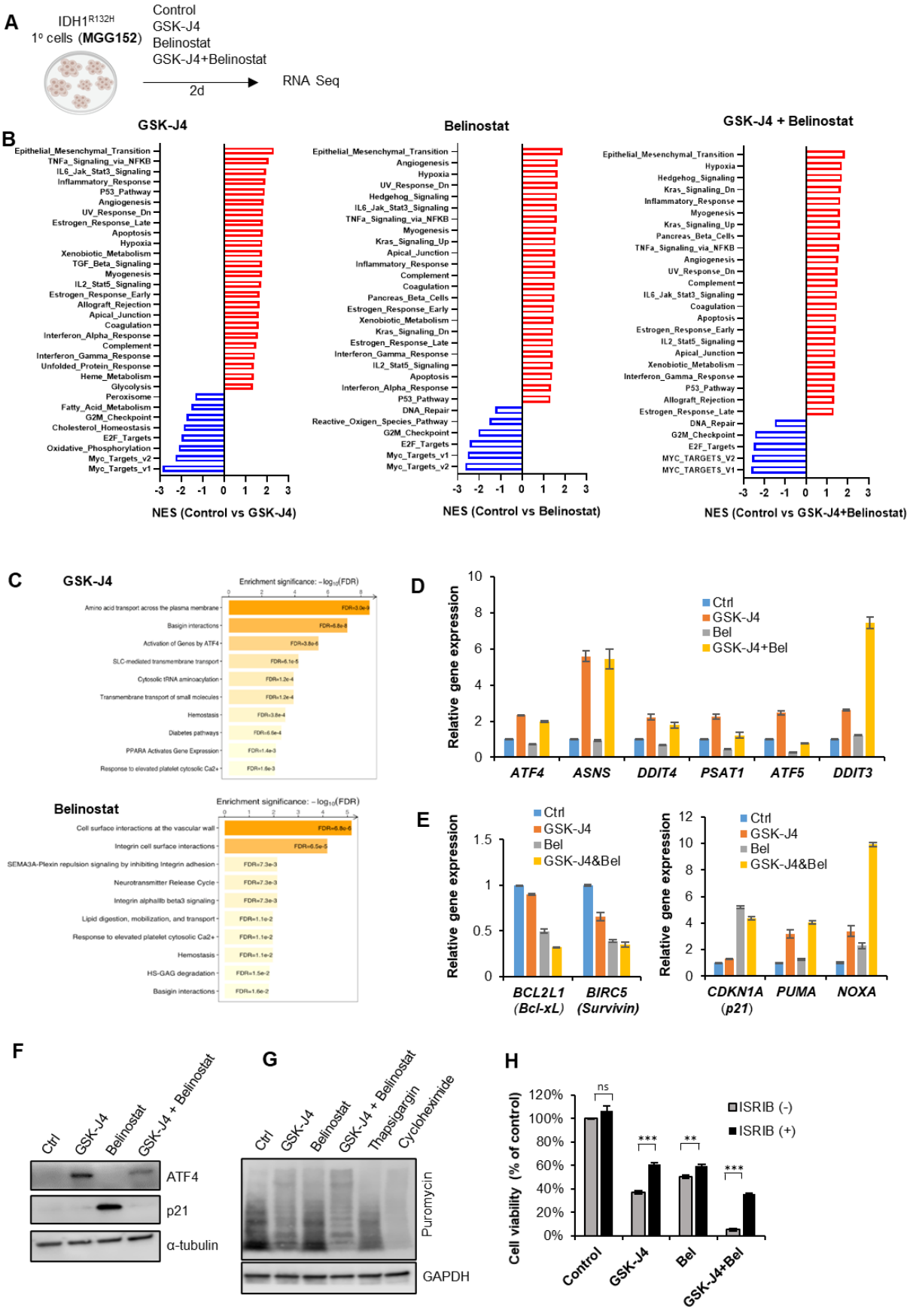

Figure 4. RNA-seq analysis on 1º *IDH1*-mutant cells reveals global changes and stress response activation upon GSK-J4 and Belinostat treatment. A) Scheme for treatment and sample collection for sequencing. **B)** GSEA output showing the hallmarks that were specifically enriched in DEGs. NES; normalized enrichment score. **C)** The bar graphs showing the top 10 enrichments in the Reactome pathways database with each compound. The false discovery rate (FDR) is displayed. **D)** The genes involved in ATF4-mediated unfolded protein response (UPR) pathway were upregulated with GSK-J4 and the combination treatment in MGG152 cells. **E)** The genes involved in apoptosis and cell cycle pathways were deregulated with GSK-J4 and Belinostat in MGG152 cells. **F)** Western blot images indicated that GSK-J4 increased ATF4 amount and Belinostat increased *CDKN1A*/p21 after 48h of treatments in MGG152 cells. **G)** SUnSET assay showing compound effects on global translation levels after 48h in MGG152 cells. GSK-J4 decreased global translation after 48h of treatment. Thapsigargin (5 µM) and cycloheximide (5 µM) were used as positive controls. **H)** ISRIB (1 µM), an inhibitor of integrated stress response pathway, partially prevented cytotoxic effects of GSK-J4 and Belinostat on MGG152 cells. p-values were determined by unpaired t test; ns, non-significant; *p < 0.05; **p < 0.01; ***p < 0.001.

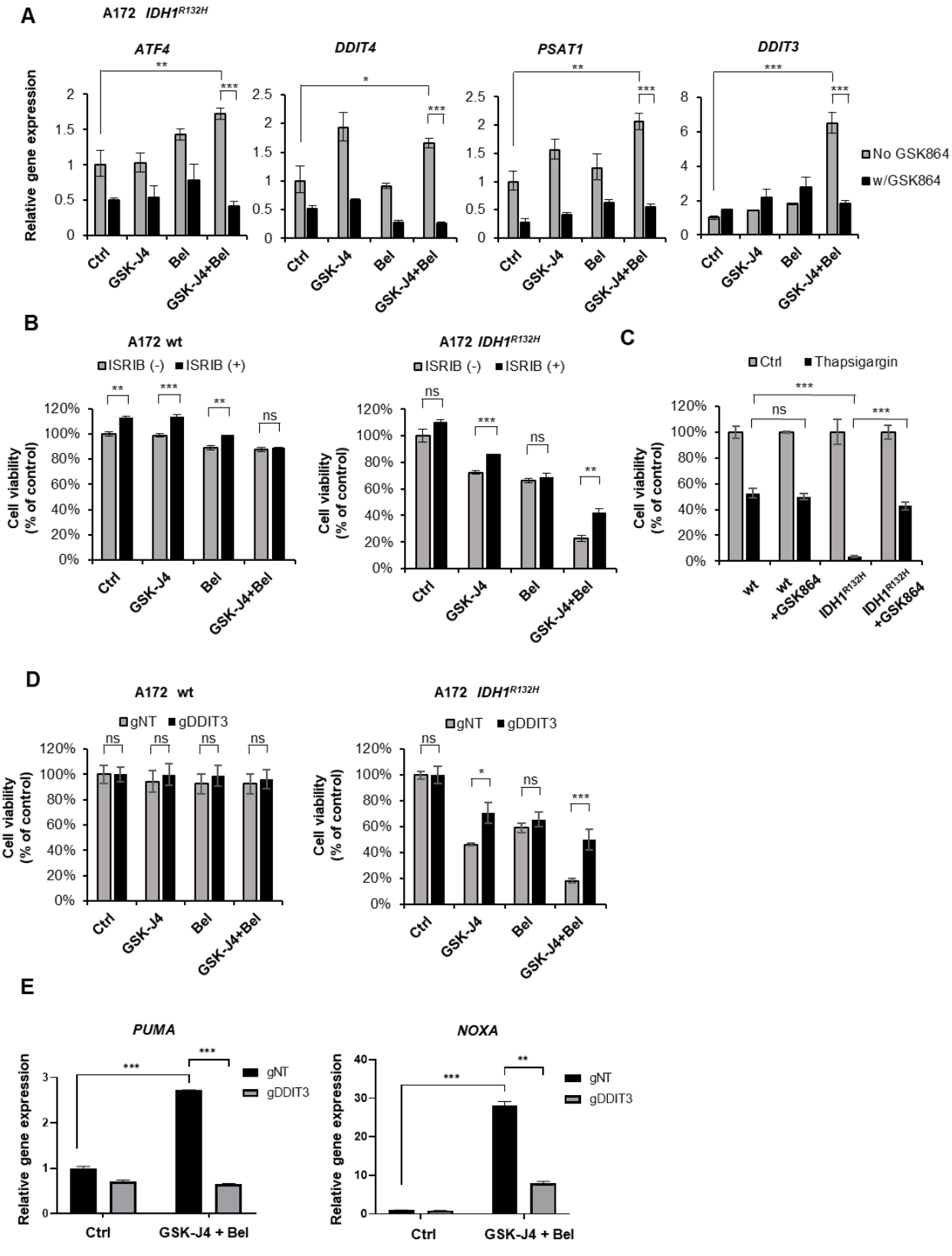

Figure 5. IDH1^{R132H} overexpression sensitizes cells to ISR mediated apoptosis induced by GSK-J4 and Belinostat combination treatment. A) Genes involved in ISR pathway were significantly upregulated with GSK-J4 and Belinostat co-treatment upon IDH1^{R132H} overexpression, and they were significantly downregulated with GSK864 (2.5 µM) pre-treatment. **B)** ISRIB (1 µM), significantly decreased cytotoxic effects of GSK-J4 individually and in combination on A172 *IDH1^{R132H}* cells. **C)** IDH1^{R132H} overexpression significantly sensitized A172 cells against Thapsigargin, an ER stress inducer, and it was recovered with GSK864 treatment. **D)** Sensitization of *IDH1^{R132H}* cells against GSK-J4 and combination treatment were significantly recovered upon inhibition of stress induced apoptosis via knock-out of *DDIT3* gene. **E)** Knock-out of *DDIT3* gene significantly inhibited activation of pro-apoptotic genes, *PMAIP1*/PUMA and *BBC3*/NOXA, upon GSK-J4 and Belinostat combination treatment. For all panels, p-values were determined by unpaired t test; ns, non-significant; *p < 0.05; **p < 0.01; ***p < 0.001.

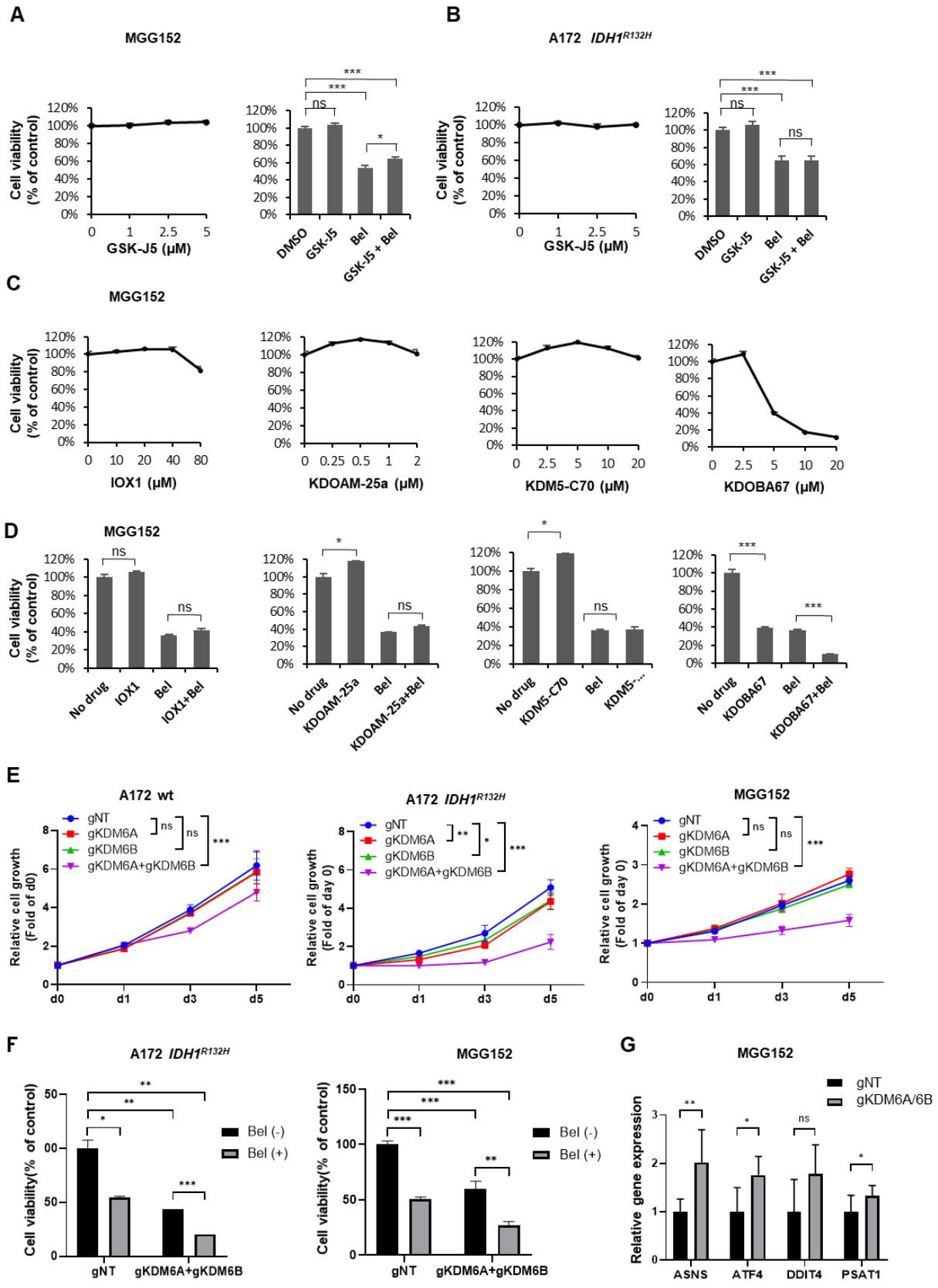

Figure 6. KDM6A and KDM6B knockdown phenocopies the effects observed with GSK-J4 in *IDH1*-mutant cells. A-B) The effect of GSK-J5, inactive form of GSK-J4, on the viability of primary *IDH1*-mutant MGG152 cells **(A)** or A172 $IDH1^{R132H}$ cells **(B),** individually or in combination with Belinostat. **C-D)** The effects of other KDM inhibitors, IOX1, KDOBA67, KDOAM-25a and KDM5-C70, on primary *IDH1*-mutant MGG152 cell viability individually **(C)** or in combination with Belinostat **(D)**. **E)** The effects of knock-out of *KDM6A* and/or *KDM6B* on the growth of A172 wild-type and A172 $IDH1^{R132H}$ cells. **F)** The effects of knock-out of *KDM6A* and/or *KDM6B* on the growth of patient-derived MGG152 cells. **G)** The effects of double knock-out of *KDM6A* and *KDM6B* and Belinostat on the viability of A172 $IDH1^{R132H}$ cells and primary MGG152 cells. **H)** The expression of stress response genes upon double knock-out of *KDM6A* and *KDM6B* in MGG152 cells. For panel F, p-values were determined by 2-way ANOVA test. For all other panels, p-values were determined by unpaired t test; ns, non-significant; *$p < 0.05$; **$p < 0.01$; ***$p < 0.001$.

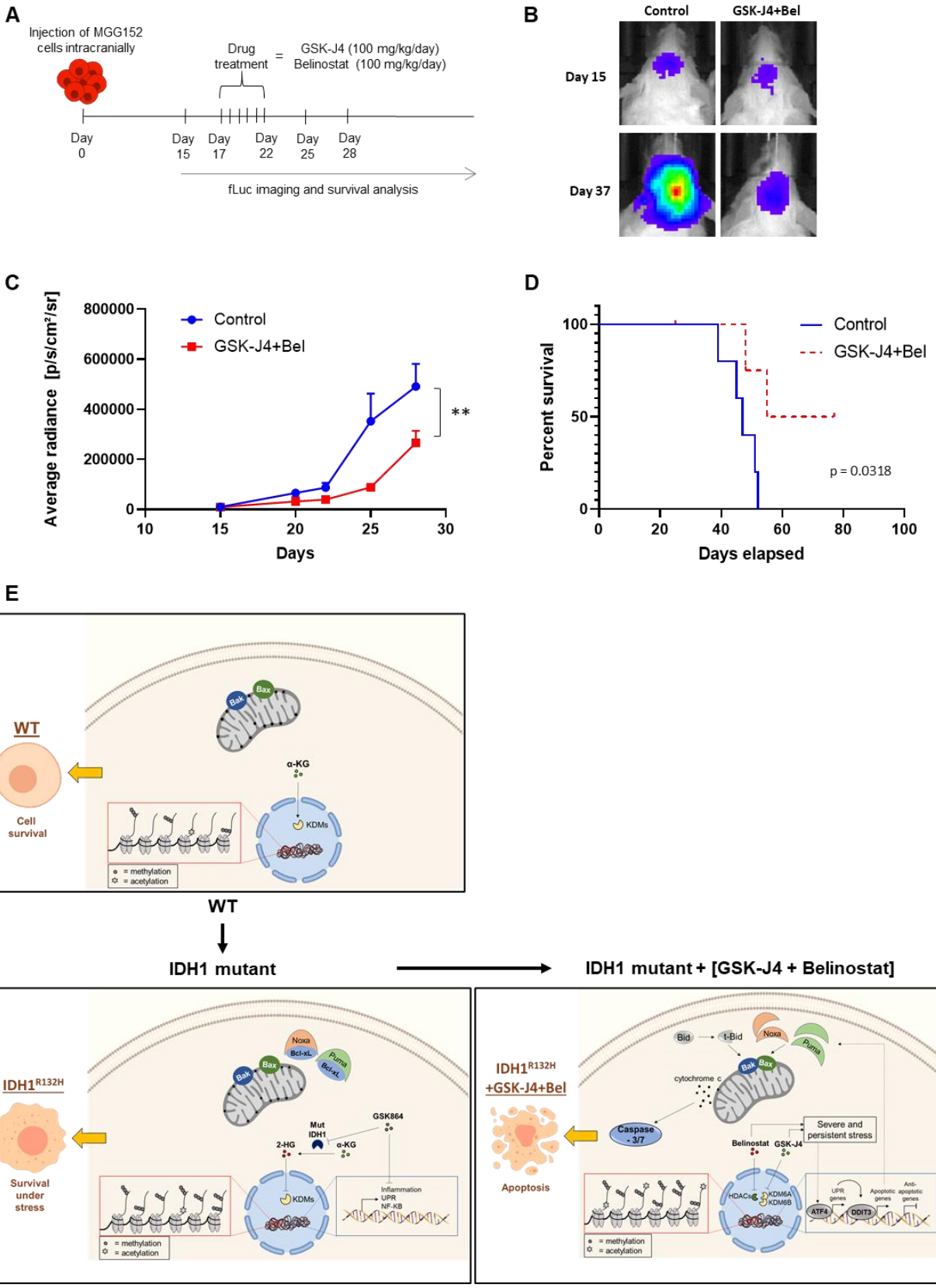

Figure 7. Effects of drug combination on *in vivo* tumor development. A) Schematic representation of timeline for *in vivo* experiments conducted with MGG152 cells. **B)** Representative images of intracranial tumors on days 15 and 37. **C)** Average radiances [p/s/cm²/sr] of control and drug treated tumors. p-value was calculated via two-way ANOVA test, *p < 0.05; **p < 0.01; ***p < 0.001. **D)** Kaplan-Meier survival plot for control and drug treated mice (n=5). p-value was calculated via Log-rank test (p=0.0318). **E)** Proposed model of the mechanism underlying the high vulnerability of *IDH1*-mutant gliomas to GSK-J4 and Belinostat combination.